Hindawi
Journal of Advanced Transportation
Volume 2022, Article ID 1716827, 11 pages
https://doi.org/10.1155/2022/1716827

Research Article

Stability Analysis of the New Traffic Flow Lattice Model considering Taillight Effect and Speed Deviation

Zhicheng Li [1] **and Changxi Ma** [2]

[1] *Department of Urban Rail Transit and Information Engineering, Anhui Communications Vocational and Technical College, Hefei 230051, China*
[2] *School of Traffic and Transportation, Lanzhou Jiaotong University, Lanzhou 730070, China*

Correspondence should be addressed to Changxi Ma; machangxi@mail.lzjtu.cn

Received 8 May 2022; Accepted 30 June 2022; Published 20 July 2022

Academic Editor: Wen Liu

A new macroscopic traffic flow lattice model is established which considered the taillight effect and velocity deviation. By combining the concept of critical density, the critical condition of taillight triggering is established. The situation of taillight appearing is fully considered, and the influence of taillight effect is analyzed. Through the stability analysis of the model, the stability conditions of the model are obtained. By nonlinear analysis, the mKdV equation is derived which can describe the evolution mechanism of the density wave. From the phase diagram, we can find that the two factors have a positive impact on the stability of traffic flow. Finally, spatiotemporal evolution of the density wave and cross-section view of the density wave are obtained by numerical simulation to verify the theoretical derivation of this paper. The simulation results show that the stability of traffic flow can be improved by considering taillight effect and speed deviation. In addition, by comparing the time-space evolution maps of different parameter values, it can be found that the stability of traffic flow considering the taillight effect and speed deviation is better than that considering one factor alone. However, the stability of traffic flow will be negatively affected by low speed estimate and high critical density.

1. Introduction

With the development of urbanization and modern science and technology, traffic problems have become the most serious social problem in recent years. Traffic jams have been one of the most serious problems. These problems not only affect the driver's psychological condition and bring safety problems but also make people waste time waiting. Therefore, in order to solve the problem of traffic congestion, scholars have put forward many methods and models to analyze in the field of transportation [1–6] including the car-following model [7–9] and lattice hydrodynamics model [10, 11]. The lattice hydrodynamic model was proposed by Nagatani [12]. He describes the evolution of traffic congestion in the form of kink-antikink density waves.

In recent years, scholars have added many new factors to the model proposed by Nagatani, making the established lattice hydrodynamics dynamics model more realistic. Kang et al. [13] established a fractional-order grey viscoelastic traffic flow model that can reflect time-varying characteristics and compared it with the traditional model. The results show that the new model has better stability and modeling effect. Wang et al. [14] designed a memory feedback control signal based on the historical traffic information of the vehicle itself to improve the intelligent driver model. The numerical simulation results show that considering the memory feedback control signal, the stability of heterogeneous traffic flow is improved no matter whether the proportion of connected vehicles is low or high. Zhao et al. [15] integrated the continuous historical flow and considered and analyzed the historical flow as a whole in view of the importance of historical flow information for stable traffic flow. Lane changing rate is involved in the two-lane lattice hydrodynamic model, and some scholars believe that setting lane changing rate as a constant is not a good choice [16]. Therefore, Zhu et al. [17] regarded lane changing rate as a variable, realized different lane changing rates in the simulation based on density changes, and found that its structure was similar to the optimal velocity equation. It is inevitable that there is a time delay in obtaining traffic information. Zhang et al. [18] proposed the factor of time-varying delay. The results showed that considering time-varying delay in actual traffic is not conducive to the stability of traffic flow. There are traffic signals and a series of other factors on the road that affect the stability of traffic flow. Therefore, Redhu and Gupta [19] studied the impact of traffic interruption probability on traffic flow. In the study of traffic flow, the influence of individual driver behavior on the stability of traffic flow is a research hotspot, such as driver prediction effect [20, 21], driver heterogeneity [22–25], and driver memory effect [26–28]. With the development of research, many scholars have applied control theory to analyze and solve the problem of traffic congestion. Through the combination analysis of delayed feedback control and multiple factors, considerable research results have been obtained [29].

Usually, the driver cannot get data such as speed and time headway. Generally speaking, drivers adjust their speed by self-estimation. In the process of driving, when the driver receives the traffic information, he will take the taillight warning of the vehicle as one of the main bases to adjust the speed in order to drive safely. However, the driver's estimation of the speed is often biased. The estimation of different speed deviations will have different effects on traffic flow. Zhou and Shi [30] proposed a full-speed difference model that took into account the velocity deviation, and the results showed that a high estimate of speed had a stabilizing effect on the traffic flow, while a low estimate of speed had a negative effect on the stability of the traffic flow. Zhang et al. [31] established a car-following model, which took into account the vehicle taillight effect. The taillight effect has been tested on circular roads and straight roads, respectively. They found that the taillight effect could effectively suppress traffic congestion problems. However, there is no research and analysis on how to trigger taillight in the above literature. Zhai and Wu [32] proposed the concept of critical density to study the honk effect. By combining the concept of critical density, a critical judgment exists as a criterion for the driver to use taillight. For the further study of the taillight effect's influence, the critical conditions for triggering taillight are set based on the critical density in this paper.

Therefore, this paper studies the effects of taillight effect and speed deviation under critical density by establishing a macro traffic flow model. The neutral stability condition of the model is obtained by linear and nonlinear analysis. In Section 2, a lattice model considering taillight effect and velocity deviation is established. In Section 3, the stability condition of the new lattice model is obtained by deducing the model with the linear analysis method. In Section 4, the reduction perturbation method is used to derive the mKdV equation and obtain the kink-antikink solution. In Section 5, the evolution diagram of the density wave near the critical point is obtained by numerical simulation based on the derived equation. In Section 6, the results of the numerical simulation are summarized and conclusions are drawn.

2. Model

In the actual driving process, the traffic information in the front and the traffic information in the rear will affect the driver. Rear traffic flow information has only a partial effect when the driver is driving. If the driver can obtain the state information of the vehicle in front of him in advance, the driver can adjust the speed of the vehicle in advance. The driver can reduce the frequency of acceleration or deceleration of the vehicle and make the speed fluctuation of the vehicle smooth. The driver's driving behavior change is mainly based on the traffic information given by the vehicle in front. And, the taillight effect can be used as the most direct traffic information. Usually, when the driver receives the taillight warning, he can judge whether the brake is needed by comparing the traffic flow density with the critical density. Therefore, the influence of taillight effect is taken into account to establish a macro traffic flow model in this paper, shown as follows:

$$\partial_t \rho_j + \rho_0 \left(\rho_j v_j - \rho_j v_j\right) = 0, \tag{1}$$

$$\partial_t \left(\rho_j v_j\right) = a\rho_0 \left[(1-p)V^F\left(\rho_{j+1}\right) + \mu p V^B\left(\rho_j\right)\right] - a\rho_j v_j, \tag{2}$$

where ρ_0 indicates average density. ρ_j and v_j are the average density and average velocity of the j^{th} lattice. a is the pilot's sensitivity. ρ_{lim} is the critical density. μ is 0–1 variables, where $\mu = \begin{cases} 0, & \rho < \rho_{\text{lim}} \\ 1, & \rho > \rho_{lim} \end{cases}$. When density $\rho < \rho_{\text{lim}}$, $\mu = 0$ means no account of taillight effect. When density $\rho > \rho_{\text{lim}}$, $\mu = 1$ means the driver will use taillights to warn vehicles behind it. p is the possibility of using taillights. It also shows drivers' attention to traffic information. In this paper, two different optimal functions are used to reflect the influence of taillight effect, in order to better fit the actual situation of the study. $V^F(\rho)$ is the function which represents the optimal velocity function under the influence of the forward density. $V^B(\rho)$ is the function which represents the optimal velocity function under the influence of the rear density. In this paper, the taillight effect is used to warn the rear traffic flow. The higher the density is, the greater the possibility of using taillights. That means the higher the density input, the smaller the value of the optimal velocity. This is the opposite of the optimal velocity function $V^F(\rho)$. ρ_c is the safety density. The specific expression is shown as follows:

$$\begin{aligned} V^F(\rho) &= \left(\frac{v_{\max}}{2}\right)\left(\left[\tanh\left(\frac{2}{\rho_0} - \frac{\rho}{\rho_0^2} - \frac{1}{\rho_c}\right) + \tanh\left(\frac{1}{\rho_c}\right)\right]\right), \\ V^B(\rho) &= \left(\frac{v_{\max}}{2}\right)\left(-\left[\tanh\left(\frac{2}{\rho_0} - \frac{\rho}{\rho_0^2} - \frac{1}{\rho_c}\right) + \tanh\left(\frac{1}{\rho_c}\right)\right]\right). \end{aligned} \tag{3}$$

In general, when the traffic flow density is higher than the critical density, the interaction between vehicles is relatively strong. In order to maintain a safe distance, the driver in front will use the taillight to warn the vehicles behind. However, when the traffic flow density is lower than the critical density, the interaction between vehicles will be reduced. Vehicles can maintain the optimal speed, and the driver in front does not need to use the taillight to warn the driver behind. Even if the front driver uses the taillight for warning, the rear driver does not need to consider the influence of the taillight. And drivers do not use the brakes as often as possible to maintain optimal speeds. Therefore, there is a possibility that the driver will use the taillights. When $p = 0$, equation (2) can be simplified as the Nagatani model.

In the normal driving process, drivers adjust their speed by self-estimation because they cannot keep their eyes on the vehicle's display. In the process of driving, the drivers get traffic information by observing other vehicles. Then, they will take the taillight warning of the vehicle ahead as one of the main bases to adjust the speed in order to drive safely. However, the driver's estimation of the speed is often biased. Therefore, in order to reflect the impact of speed deviation and the taillight on traffic flow, equation (2) is rewritten into the following form:

$$\partial_t\left(\rho_j v_j\right) = a\rho_0\left[(1-p)V^F\left(\rho_{j+1}\right) + \mu p V^B\left(\rho_j\right)\right] - a(1+k)\rho_j v_j. \tag{4}$$

Here, k represents the deviation degree of speed v. When $p = 0$ and $k = 0$, equation (2) can be simplified as the Nagatani model.

According to equations (1) and (4), the velocity term is eliminated, and equation (5) is obtained as follows:

$$\begin{aligned}&\partial_t^2\rho_j + a\rho_0^2\left[V^F\left(\rho_{j+1}\right) - V^F\left(\rho_j\right)\right](1-p)+\\&a\rho_0^2\mu\left[V^B\left(\rho_j\right) - V^B\left(\rho_{j-1}\right)\right]p + a(1+k)\partial_t\rho_j = 0.\end{aligned} \tag{5}$$

3. Linear Analysis

In order to study the excessive interference of taillight effect and velocity deviation on traffic flow in this paper, the linear stability theory is applied to solve the stability condition of the model. Assume that the initial traffic flow on the road is in a uniform and stable state. There are constant density ρ_0 and optimal speed $V(\rho_0)$. The steady-state solution of the model is as follows:

$$\begin{aligned}\rho_j(t) &= \rho_0,\\ v_j(t) &= V(\rho_0).\end{aligned} \tag{6}$$

Set $y_j(t)$ as a small disturbance in the steady-state density of the j^{th} lattice. $\rho_j(t) = \rho_0 + y_j(t)$ means adding a small disturbance in the steady-state density. And, $y_j(t)$ can be defined as $y_j(t) = \exp(ikj + zt)$. Therefore,

$$\begin{aligned}\partial_t\rho_j &= z y_j(t),\\ \partial_t^2\rho_j &= z^2 y_j(t),\\ V\left(\rho_j\right) &= V(\rho_0) + V'(\rho_0)y_j(t),\end{aligned} \tag{7}$$

where $V^{F\prime}(\rho_0) = (\mathrm{d}V^F(\rho)/\mathrm{d}\rho)|\rho = \rho_0$ and $V^{B\prime}(\rho_0) = (\mathrm{d}V^B(\rho)/\mathrm{d}\rho)|\rho = \rho_0$. Substituting the previous formula into the simplified formula, we can get

$$\begin{aligned}&z^2 + a(1+k)z + a\rho_0^2 V^{F\prime}(\rho_0)\left(e^{ik} - 1\right)(1-p)\\&+ a\rho_0^2\mu V^{B\prime}(\rho_0)\left(1 - e^{-ik}\right)p = 0.\end{aligned} \tag{8}$$

Inserting $z = z_1 ik + z_2(ik)^2 + \cdots$ into equation (7), we can obtain

$$\begin{aligned}&-z_1^2k^2 + a(1+k)z_1 ik - a(1-r)(1+k)z_2k^2\\&+ a\rho_0^2 V^{F'}(\rho_0)\left(ik - \frac{1}{2}k^2\right)\\&(1-p) + a\rho_0^2\mu V^{B'}(\rho_0)\left(ik + \frac{1}{2}k^2\right)p = 0.\end{aligned} \tag{9}$$

By calculating the first-order and second-order coefficients in z, we can get the following equations:

$$z_1 = -\frac{\rho_0^2\left[V^{F\prime}(\rho_0)(1-p) + \mu V^{B\prime}(\rho_0)p\right]}{(1+k)}, \tag{10}$$

$$\begin{aligned}z_2 = &-\frac{\rho_0^4\left[V^{F\prime}(\rho_0)(1-p) + \mu V^{B\prime}(\rho_0)p\right]^2}{a(1+k)^3}\\&-\frac{\rho_0^2\left[V^{F\prime}(\rho_0)(1-p) - \mu V^{B\prime}(\rho_0)p\right]}{2(1+k)}.\end{aligned} \tag{11}$$

According to the theory of stability, when $z_2 < 0$, after a long-wave disturbance, smaller uniform traffic flow will become unstable. If the same situation occurs with $z_2 > 0$, traffic flow is still stable and neutral stability conditions can be expressed as

$$a = \frac{-2\rho_0^2\left[V^{F\prime}(\rho_0)(1-p) + \mu V^{B\prime}(\rho_0)p\right]^2}{(1+k)^2\left[V^{F\prime}(\rho_0)(1-p) - \mu V^{B\prime}(\rho_0)p\right]}. \tag{12}$$

When $p = 0$ and $k = 0$, the stability condition in this paper and the stability condition proposed by Nagatani are consistent.

The solid and dashed lines represent coexistence and neutral stability curves, respectively. The solid and dashed lines of the same color in Figure 1 correspond to the same parameter value. The curve in the figure divides the space into a stable region, metastable region, and unstable region. In Figure 1, the parameter is set as $v_{\max} = 2$ and

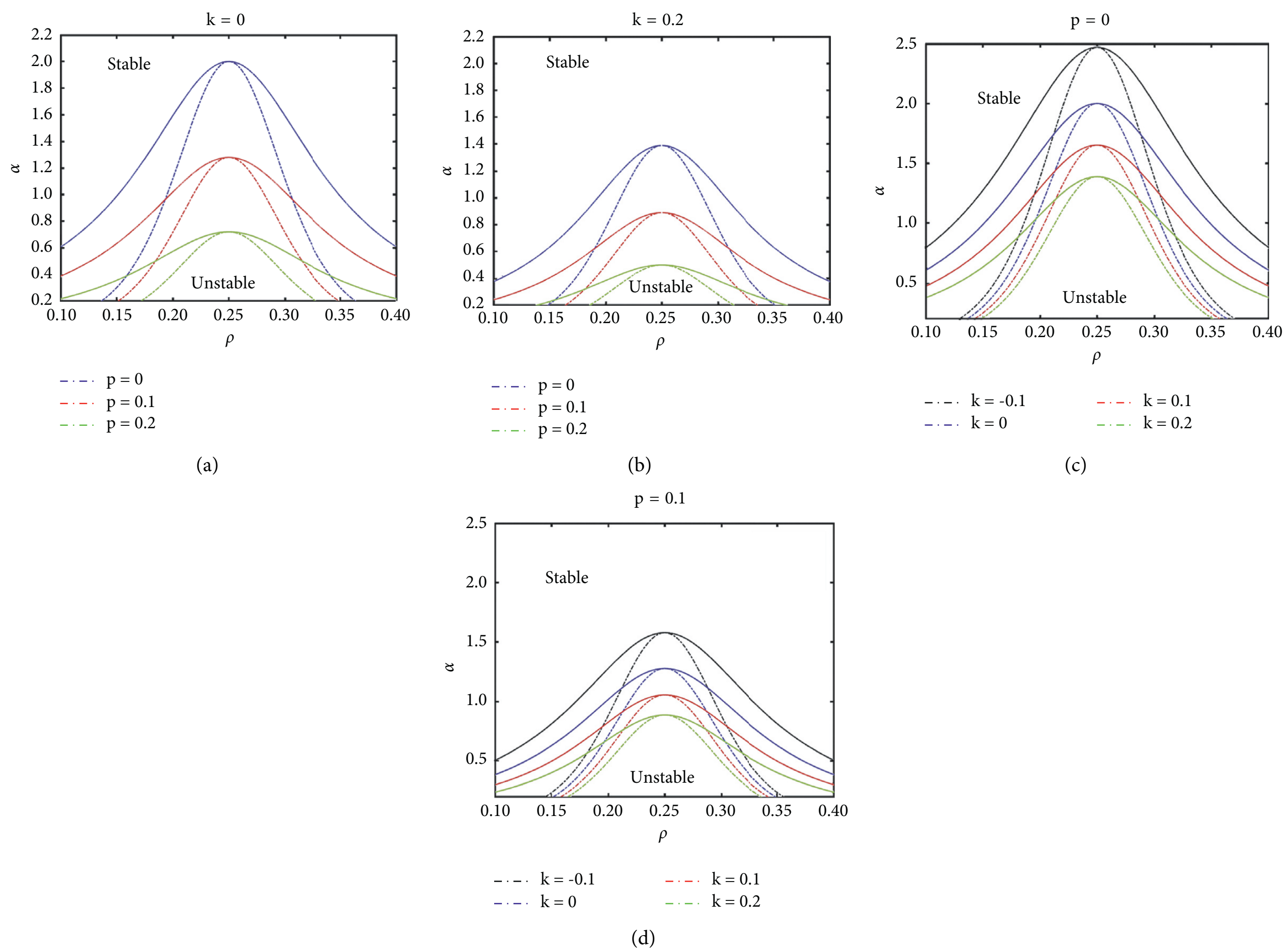

FIGURE 1: Phase diagram in parameter space (ρ, a). (a) $k=0$. (b) $k=0.2$. (c) $p=0$. (d) $p=0.1$.

$\rho_c = \rho_0 = 0.25$. The area of the stability region increased with the increase in weight coefficient p constantly in Figure 1(a) without considering speed deviation value of this effect. This means that considering the taillight effect has a positive effect on the stability of traffic flow and can improve the stability of traffic flow. Figure 1(b) shows that the taillight effect is considered as well as the speed deviation. The comparison between Figures 1(a) and 1(b) shows that the coexistence curve and the neutral stability curve in Figure 1(b) are lower than those in Figure 1(a). This shows that the taillight effect can make the stability of traffic flow get bigger promotion under the influence of speed deviation k. Figure 1(c) only considers the influence of the velocity deviation. When k takes a negative value, it can be proved that a low-speed estimator is not conducive to the stability of traffic flow. When k takes positive value, the curve of the wave is lower with the increase in k. It suggests that a high-speed estimator can increase traffic flow stability. Comparing Figures 1(c) and 1(d), it can be found with the increase of weight p, speed deviation can further expand the influence of the stability region. Therefore, considering taillight effect and speed deviation can improve the stability of traffic flow to a greater extent.

4. Nonlinear Analysis

By using the reduced perturbation method and long-wave expansion, the mKdV equation describing traffic congestion near the critical point can be obtained. The mKdV equation near the critical point can show the kink wave better. Firstly, the slow-changing behavior of spatial and temporal variables is defined as slow variables X and T for $0 < \epsilon \leq 1$, and it can be expressed as follows:

$$\begin{aligned} X &= \varepsilon (j + bt), \\ T &= \varepsilon^3 t, \\ \rho_j &= \rho_c + \varepsilon R(X, T). \end{aligned} \tag{13}$$

Substituting the slow variables X and T and equation (12) into equations (4) and (12), we can get the following by taking the Taylor expansions with the fifth order of ε:

$$\varepsilon^2\left(ab(1+k)+a\rho_0^2\left[V^{F\prime}(\rho_c)(1-p)+\mu V^{B\prime}(\rho_c)p\right]\right)\partial_x R$$
$$+\varepsilon^3\left(b^2+\frac{a\rho_0^2}{2}\left[V^{F\prime}(\rho_c)(1-p)-\mu V^{B\prime}(\rho_c)p\right]\right)\partial_X^2 R$$
$$+\varepsilon^4\left(a(1+k)\partial_T R+\frac{a\rho_0^2}{6}\left[V^{F\prime\prime\prime}(\rho_c)(1-p)+\mu V^{B\prime\prime\prime}(\rho_c)p\right]\partial_X R^3\right.$$
$$\left.+\frac{a\rho_0^2}{6}\left[V^{F\prime}(\rho_c)(1-p)+\mu V^{B\prime}(\rho_c)p\partial_X^3 R\right)$$
$$+\varepsilon^5\left(2b\partial_T\partial_X R+\frac{a\rho_0^2}{12}\left[V^{F'''}(\rho_c)(1-p)-\mu V^{B'''}(\rho_c)p\right]\partial_X^2 R^3\right.$$
$$\left.+\frac{a\rho_0^2}{24}\left[V^{F'}(\rho_c)(1-p)-\mu V^{B'}(\rho_c)p\right]\partial_X^4 R\right)=0. \tag{14}$$

Here, $V^{F\prime}=\mathrm{d}V(\rho)/\mathrm{d}\rho|\rho=\rho_c$ and $V^{F}=\mathrm{d}^3V(\rho)/\mathrm{d}\rho^3|\rho=\rho_c$. Near the critical point, we have $a_c=a(\varepsilon^2+1)$. Assuming $b=-\rho_0^2[V^{F\prime}(\rho_0)(1-p)+\mu V^{B\prime}(\rho_0)p]/(1+k)$ and eliminating the second-order and third-order terms of equation (14), we obtain

$$\begin{aligned}&\varepsilon^4\left(\partial_T R-g_1\partial_X^3 R+g_2\partial_X R^3\right)\\&+\varepsilon^5\left(g_3\partial_X^2 R+g_4\partial_X^4 R+g_5\partial_X^2 R^3\right)=0.\end{aligned} \tag{15}$$

The coefficients $g_i\,(i=1,2,\cdots 5)$ of equation (15) are listed in Table 1.

Taking the transformations $R=\sqrt{g_1/g_2}R'$ and $T'=g_1T$ into equation (14), the standard mKdV equation with an $O(\varepsilon)$ correction term is as follows:

$$\partial_{T'}R'-\partial_X^3R'+\partial_X R'^3+\varepsilon M[R']=0, \tag{16}$$

where $M[R']=1/g_1\,(g_3\partial_X^2R'+g_1g_5/g_2\partial_X^2R'^3+g_4\partial_X^4R')$.

Ignoring the $O(\varepsilon)$ term in equation (16), the kink-antikink solution of the mKdV equation can be obtained:

$$R_0'(X,T')=\sqrt{c}\tanh\left[\sqrt{\frac{c}{2}}\,(X-cT')\right], \tag{17}$$

when $R_0'(X,T')=R_0'(X,T')+\varepsilon R_1'(X,T')$. When the same condition is satisfied, the propagation velocity c can be gained by using the following formula:

$$c=\frac{5g_2g_3}{2g_2g_4-3g_1g_5}. \tag{18}$$

The kink and antikink solution of the mKdV equation is obtained as follows:

$$\rho_j=\rho_c+\varepsilon\sqrt{\frac{g_1c}{g_2}}\tanh\left[\sqrt{\frac{c}{2}}\,(X-cg_1T)\right], \tag{19}$$

where $a=-2\rho_0^2[V^{F\prime}(\rho_0)(1-p)+\mu V^{B\prime}(\rho_0)p]/(1-r)^2(1+k)^2[V^{F\prime}(\rho_0)(1-p)-\mu V^{B\prime}(\rho_0)p]$ and $\varepsilon^2=a_c/a-1$. The amplitude A of the solution is

$$A=\sqrt{\frac{g_1}{g_2}\varepsilon^2c}. \tag{20}$$

The kink-antikink solution means the road exists with coexisting traffic patterns, including low density (free-flow phase) and high density (jammed phase). The low density is $\rho=\rho_c-A$ and high density is $\rho=\rho_c+A$, which correspond to the coexistence curve in Figure 1.

5. Numerical Simulation

For the convenience of numerical simulation, equation (4) is rewritten into the form of a difference equation:

$$\begin{aligned}\rho_j(t+2\tau)=2\rho_j(t+\tau)-\rho_j(t)\\-a(1+k)\tau\left(\rho_j(t+\tau)-\rho_j(t)\right)\\-a\rho_0^2\tau^2\left(V^F\left(\rho_{j+1}(t)\right)-V^F\left(\rho_j(t)\right)\right)(1-p)\\-a\rho_0^2\tau^2\mu\left(V^B\left(\rho_j(t)\right)-V^B\left(\rho_{j-1}(t)\right)\right)p,\end{aligned} \tag{21}$$

where τ is the time step. For the optimal speed function V, the parameter is set to $v_{\max}=2$ and $\rho_c=\rho_0=0.25$. Under the condition of periodic boundary, the initial condition of numerical simulation is to set the number of lattices as $N=100$. The initial density is a piecewise function.

$$\begin{aligned}&\rho_j(\tau)=\begin{cases}\rho_0+\Delta\rho, & j=50\\ \rho_0-\Delta\rho, & j=49\,,\\ \rho_0, & \text{otherwise}\end{cases}\\&\rho_j(0)=\rho_0=0.25\,(j=1,2,\ldots N),\end{aligned} \tag{22}$$

where ρ is the initial disturbance, where $\rho=0.03$. And, the sensitivity is $a=1.6$.

5.1. The Influence of Parameter p. The parameters set in this paper are the unsteady state of traffic flow. The small disturbance added in the space will not be absorbed, but it will make the traffic flow unstable with the passage of time and form a triggered stop-and-go wave. Figure 2 shows the density time-space variation diagram and density wave cross-section diagram under the influence of different parameters p at $t=10,000\sim 10,300$ s. In Figure 2(a), it can be seen that the added small disturbance has not been absorbed and formed a blockage. Here, the taillight effect is considered as a separate factor. As the parameter p increased, the density-wave amplitude is smaller. When $p=0.2$, traffic flow stability condition is met. Traffic flows back to a steady state. Therefore, the taillight effect can effectively restrain the congestion of traffic flow and improve the stability of traffic flow.

It can be seen that the disturbance will propagate in the system with the evolution of time from Figure 2(f) after it is

Table 1: The coefficients of equation (15).

g_1	$-\rho_0^2/6\,(V^{F'}(\rho_c)(1-p)+\mu V^{B'}(\rho_c)p)$
g_2	$\rho_0^2/6\,(V^{F'''}(\rho_c)(1-p)+\mu V^{B'''}(\rho_c)p)$
g_3	$-\rho_0^2/2\,(V^{F'}(\rho_c)(1-p)-\mu V^{B'}(\rho_c)p)$
g_4	$\rho_0^2/24\,[V^{F'}(\rho_c)(1-p)-\mu V^{B'}(\rho_c)p]+\rho_0^4/3\,(1+k)a_c\,(V^{F'}(\rho_c)(1-p)+\mu V^{B'}(\rho_c)p)^2$
g_5	$\rho_0^2/12\,(V^{F'''}(\rho_c)(1-p)-\mu V^{B'''}(\rho_c)p)+\rho_0^4/3a_c\,(V^{F'}(\rho_c)(1-p)+\mu V^{B'}(\rho_c)p)(V^{F'''}(\rho_c)(1-p)+\mu V^{B'''}(\rho_c)p)$

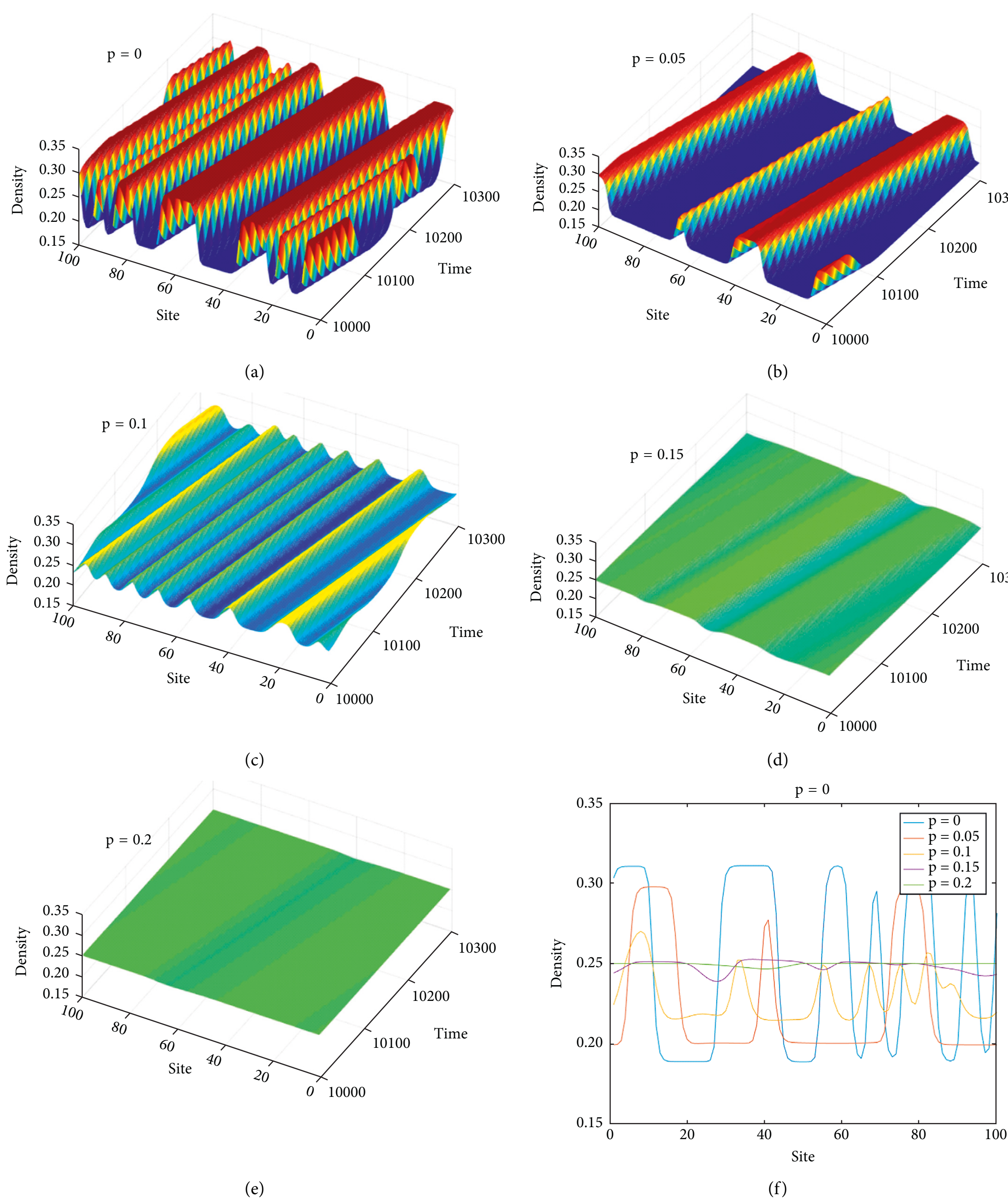

Figure 2: Spatiotemporal evolution of the density wave and cross-section view of the density wave with time under the action of different p. (a) $p=0$. (b) $p=0.05$. (c) $p=0.1$. (d) $p=0.15$. (e) $p=0.2$. (f) $p=0$.

Table 2: Fluctuation amplitude of traffic flow density with different values of parameter p at $t = 10,300$ s.

Parameter p	ρ_{max}	Fluctuation amplitude (%)	ρ_{min}	Fluctuation amplitude (%)
$p = 0$	0.3109	24.36	0.1891	24.36
$p = 0.05$	0.2977	19.08	0.1996	20.16
$p = 0.1$	0.2702	8.08	0.2150	14
$p = 0.15$	0.2527	1.08	0.2390	4.4
$p = 0.2$	0.2501	0.04	0.2468	1.28

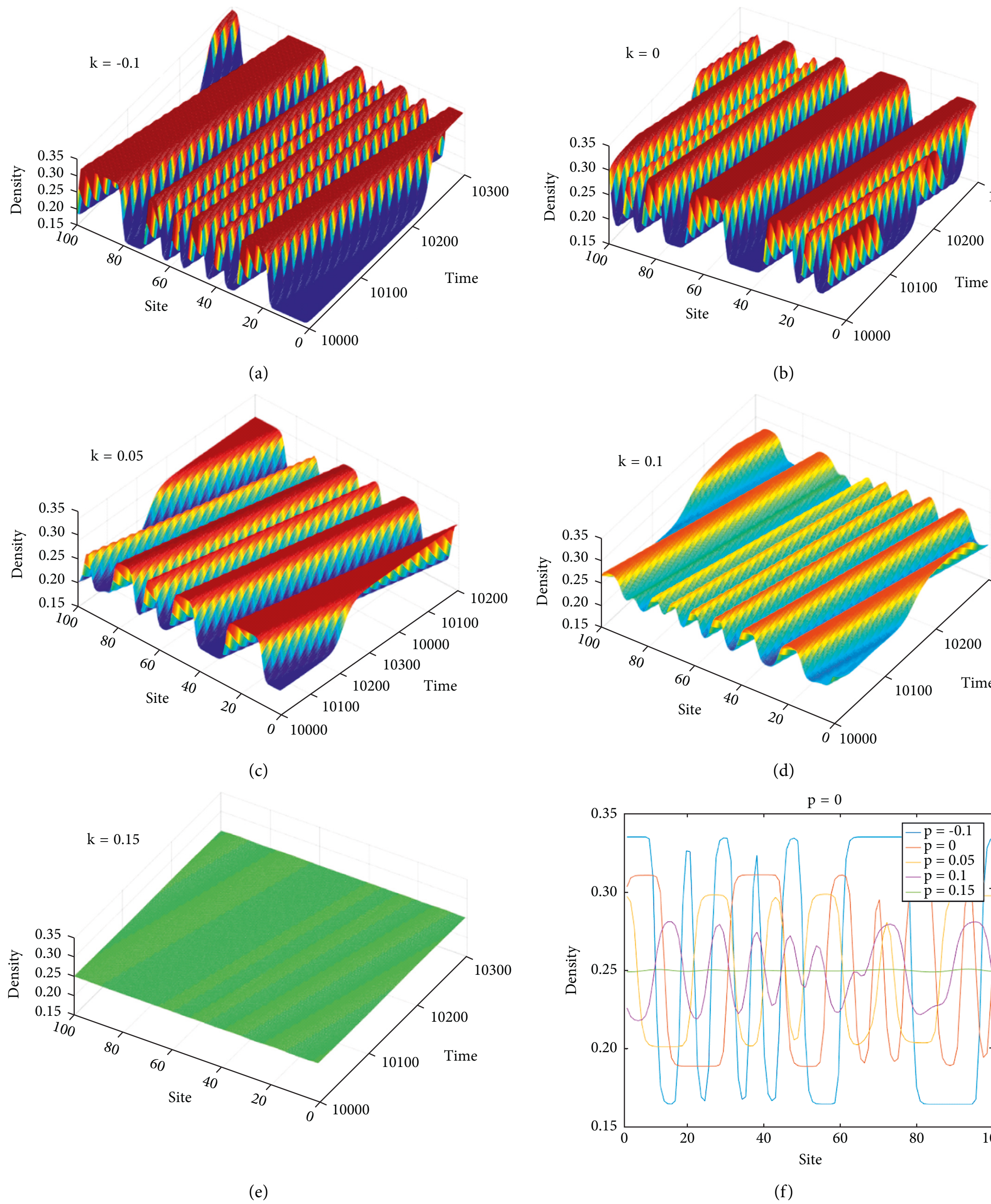

Figure 3: Spatiotemporal evolution of the density wave and cross-section view of the density wave with time under the action of different k. (a) $k = 0.1$. (b) $k = 0$. (c) $k = 0.05$. (d) $k = 0.1$. (e) $k = 0.15$. (f) $p = 0$.

Table 3: Fluctuation amplitude of traffic flow density with different values of parameter k at t = 10300 s.

Parameter p	ρ_{max}	Fluctuation amplitude (%)	ρ_{min}	Fluctuation amplitude (%)
$k = -0.1$	0.3350	34	0.1650	34
$k = 0$	0.3109	24.36	0.1891	24.36
$k = 0.05$	0.2985	19.40	0.2017	19.32
$k = 0.1$	0.2812	12.48	0.2182	12.72
$k = 0.15$	0.2509	0.36	0.2491	0.36

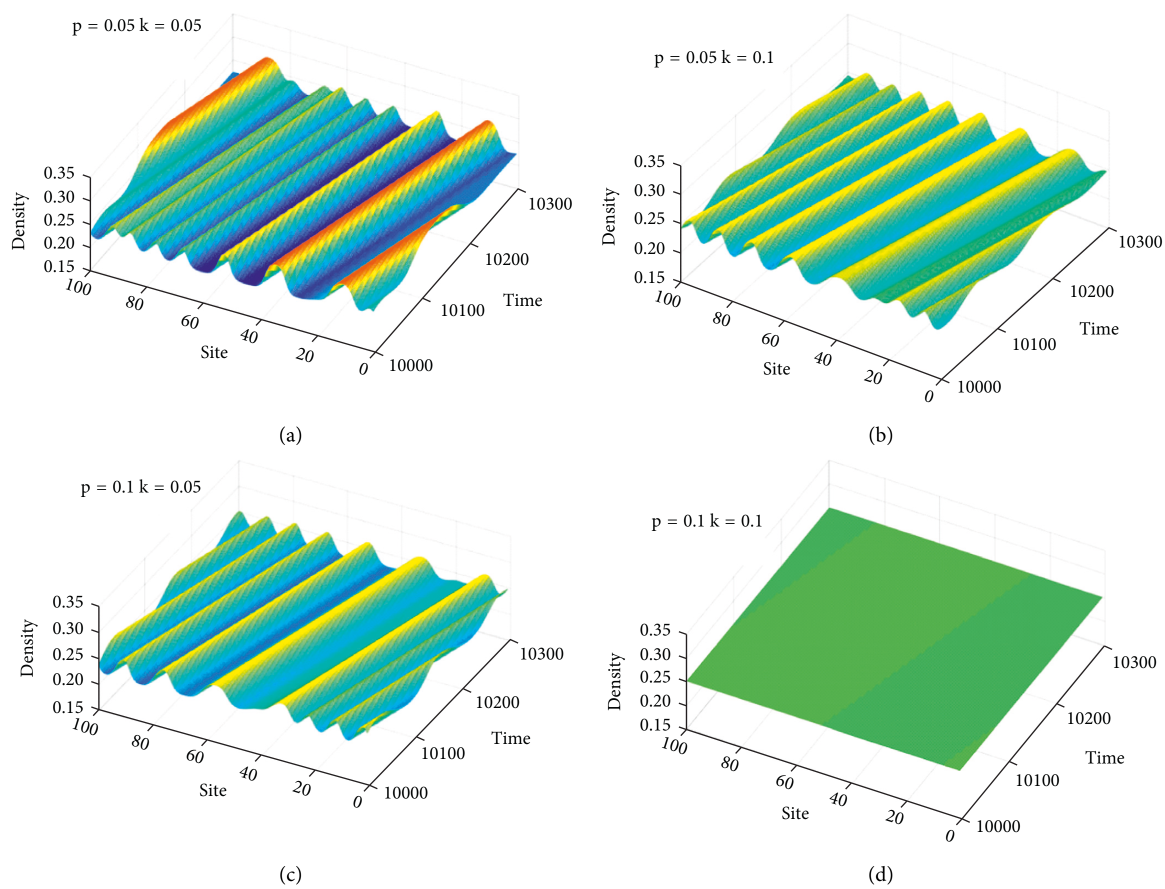

Figure 4: Spatiotemporal evolution of the density wave with time under the action of different parameters. (a) $p = 0.05$, $k = 0.05$. (b) $p = 0.05$, $k = 0.1$. (c) $p = 0.1$, $k = 0.05$. (d) $p = 0$, $k = 0.1$.

added to the stable traffic flow system. But with the increase in parameter p, the amplitude is decreasing. This also means that the traffic flow tends to be stable gradually with the increasing possibility of using taillights. Combined with Table 2 and Figure 2(f), it can be found that the maximum density of the model is 0.3109 and the fluctuation amplitude relative to the initial density is 24.36%; the minimum density is 0.1891, and the fluctuation amplitude relative to the initial density is 24.36%. When $p = 0.1$, the maximum density of the system is 0.2702 and the fluctuation range is 8.08% compared with the initial density; the minimum density is 0.2150, and the fluctuation amplitude relative to the initial density is 14%. At this time, the fluctuation amplitude of the system is obviously reduced compared with that of $p = 0$. When $p = 0.2$, the maximum density of the system is 0.2501 and the fluctuation range is 0.04% compared with the initial density; the maximum density is 0.2468, and the fluctuation range is 1.28% compared with the initial density. At this time, the fluctuation amplitude is very small compared with the initial density and the state of traffic flow is almost close to uniform flow.

5.2. Influence of Parameter k. Figure 3 shows the spatial-temporal evolution of the density wave and cross section of the density wave under the influence of different parameters k at t = 10000 ~ 10300 s. When the velocity deviation k is negative, it means that the estimation of velocity is low. From Figures 3(a) and 3(f), it can be seen that the low-speed estimate is not conducive to the stability of traffic flow. From Figures 3(b) to 3(e), it can be found that when k is positive, the amplitude of traffic flow decreases and tends to be stable with the increase in speed deviation k. When $k = 0.15$, the traffic flow is stable. Therefore, it can be concluded that the

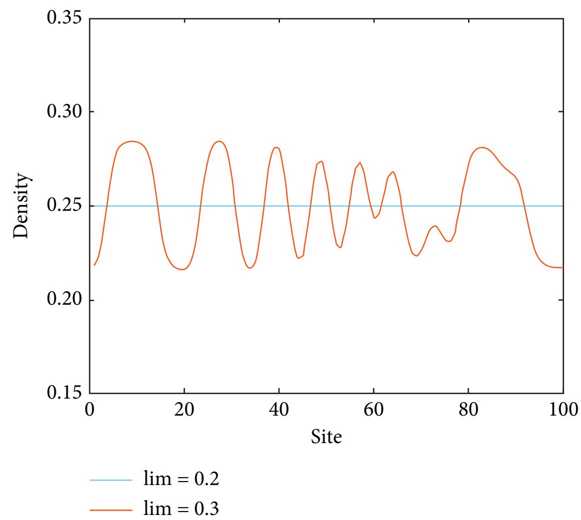

Figure 5: Cross-section view of the density wave with time under the action of different ρ_{lim}.

low-speed estimate is bad for the stability of traffic flow, while the high-speed estimate plays an important role in the stability of traffic flow.

Combining Table 3 with Figure 3(f), it can be found that the amplitude is decreasing with the increase in parameter k. This also means that with the increase in speed estimation, the unstable traffic flow is transforming to a stable state. When $k = -0.1$, the fluctuation amplitude of the maximum and minimum density of the model is 34% compared with the initial density and the density fluctuates between 0.1650 and 0.3350. Compared with the Nagatani model ($k = 0$), it can be found that a low-speed estimate is bad for the stability of traffic flow. When $k = 0.05$, the maximum density of the system is 0.2985, with a fluctuation amplitude of 19.40% compared with the initial density. The minimum density is 0.2017, and the fluctuation amplitude relative to the initial density is 19.32%. At this time, the fluctuation amplitude of the system is significantly reduced compared with that of $k = -0.1$. When $k = 0.15$, the fluctuation amplitude of the model relative to the initial density is 0.36% and the density fluctuates between 0.2491 and 0.2509. At this time, the density difference compared with the initial density is 0.0009, which shows that the higher the speed estimate, the more stable the traffic flow.

5.3. Influence of Parameter $p - k$. Figure 4 shows the spatiotemporal evolution of parameters p and k under different values at $t = 10000 \sim 10300$ s. Through the comparison between Figures 2(b) and 4(a), it can be found that when the parameter p is taken as 0.05 at the same time, the amplitude of the density wave in Figure 4(a) is more stable when $k = 0.05$ than that in Figure 2(b) when $k = 0$. In addition, it can be further proved from Figure 4(b) that high-speed estimators play a role in stabilizing traffic flow. When the parameters $p = 0.1$ and $k = 0.1$ in Figure 4(d), the traffic flow reaches a stable state. However, when $p = 0.2$ and $k = 0.15$, the traffic flow is stable in Figures 2(e) and 3(e). Therefore, it can be concluded that considering the taillight effect and the high-speed estimator can stabilize traffic flow.

5.4. Influence of Parameter ρ_{lim}. In this paper, the critical density is used as the trigger condition of the taillight. The selection of critical density parameters has a certain influence on the results. In order to analyze the influence of this feature on traffic flow, Figure 5 shows the cross-section view of density waves under different critical densities when $t = 10300$ s. The parameters are set as $p = 0.1$ and $k = 0.1$. At this time, the traffic flow is in a stable state. In the above simulation process, the critical density $\rho_{\text{lim}} = 0.25$ has reached a stable state. When the critical density ρ_{lim} is close to 0, the more likely it is for the driver to consider the taillight effect and the more stable the traffic flow will be. In Figure 5, the parameters are set as $\rho_{\text{lim}} = 0.2$ and $\rho_{\text{lim}} = 0.3$, respectively. When the critical density is lower than 0.25, the more likely it is for the driver to perform the taillight operation, which means that the traffic flow will remain stable all the time. In Figure 5, it can be found that when the critical density ρ_{lim} becomes larger, the density wave will oscillate. This means that a larger critical density is not conducive to the stability of traffic flow.

6. Conclusions

In this paper, the evolution form of macro traffic flow under the environment of vehicle road communication is taken as the research object. In this paper, the taillight effect and velocity deviation are taken into account and a new lattice hydrodynamic model is established. In addition, with the concept of critical density, critical conditions are set for the taillight effect, which makes the case of triggering taillight more comprehensive. The stability conditions of the model are obtained by linear stability analysis. The nonlinear analysis is carried out by the reduction perturbation method, and the kink-antikink wave is obtained by the mKdV equation. The propagation behavior of the traffic density wave at the critical point is revealed by the phase diagram. Finally, the theory of the model is verified by numerical simulation. The simulation results show that the taillight effect combined with the critical density and the speed deviation can effectively restrain the traffic jam. The stability of traffic flow can be enhanced by increasing the possibility of considering taillights and reducing the critical density. The high-speed estimate plays a stable role in the traffic flow, while the low-speed estimate will reduce the stability of the traffic flow. Through the comparison of the combination of multiple parameters, the taillight effect and the speed deviation can be considered more effectively to make the traffic flow reach a stable state. The simulation results are consistent with the theoretical analysis. However, the limitations of this paper are that the drivers are regarded as homogeneous, different drivers have different cognitions of speed and critical density, and their psychological behaviors are also different. Therefore, this research will be the direction of follow-up research.

Data Availability

The data used to support the findings of this study are available from the corresponding author upon request.

Conflicts of Interest

The authors declare that they have no conflicts of interest.

Acknowledgments

This research was jointly funded by the 2022 Anhui Province University Outstanding Talent Cultivation Project, Natural Science Foundation of Anhui Province (Nos. KJ2020A1064 and KJ2021A1472), and Quality Engineering of Anhui Province (Nos. 2020szsfkc030 and 2020zyq24).

References

[1] J. Tang, J. Liang, C. Han, Z. Li, and H. Huang, "Crash injury severity analysis using a two-layer Stacking framework," *Accident Analysis & Prevention*, vol. 122, pp. 226–238, 2019.

[2] J. Tang, Y. Yang, and Y. Qi, "A hybrid algorithm for urban transit schedule optimization," *Physica A: Statistical Mechanics and Its Applications*, vol. 512, pp. 745–755, 2018.

[3] J. Tang, J. Liang, S. Zhang, H. Huang, and F. Liu, "Inferring driving trajectories based on probabilistic model from large scale taxi GPS data," *Physica A: Statistical Mechanics and Its Applications*, vol. 506, pp. 566–577, 2018.

[4] W. Wu, R. Liu, and W. Jin, "Designing robust schedule coordination scheme for transit networks with safety control margins," *Transportation Research Part B: Methodological*, vol. 93, pp. 495–519, 2016.

[5] W. Wu, R. Liu, W. Jin, and C. Ma, "Stochastic bus schedule coordination considering demand assignment and rerouting of passengers," *Transportation Research Part B: Methodological*, vol. 121, pp. 275–303, 2019.

[6] W. Wu, R. Liu, and W. Jin, "Modelling bus bunching and holding control with vehicle overtaking and distributed passenger boarding behaviour," *Transportation Research Part B: Methodological*, vol. 104, pp. 175–197, 2017.

[7] C. Zhai and W. Wu, "An extended multi-phase lattice model with consideration of optimal current changes with memory," *Cluster Computing*, vol. 22, pp. 7447–7457, 2019.

[8] J. Wang, F. Sun, R. Cheng, H. Ge, and Q. Wei, "An extended car-following model considering random safety distance with different probabilities," *Modern Physics Letters B*, vol. 32, no. 05, Article ID 1850056, 2018.

[9] Y. Sun, H. Ge, and R. Cheng, "An extended car-following model considering driver's memory and average speed of preceding vehicles with control strategy," *Physica A: Statistical Mechanics and Its Applications*, vol. 521, pp. 752–761, 2019.

[10] X. Qi, R. Cheng, and H. Ge, "Nonlinear analysis of a new two-lane lattice hydrodynamic model accounting for "backward looking" effect and relative flow information," *Modern Physics Letters B*, vol. 33, no. 19, Article ID 1950223, 2019.

[11] C. Jiang, R. Cheng, and H. Ge, "Mean-field flow difference model with consideration of on-ramp and off-ramp," *Physica A: Statistical Mechanics and Its Applications*, vol. 513, pp. 465–476, 2019.

[12] T. Nagatani, "Modified KdV equation for jamming transition in the continuum models of traffic," *Physica A: Statistical Mechanics and Its Applications*, vol. 261, no. 3-4, pp. 599–607, 1998.

[13] Y. Kang, S. Mao, and Y. Zhang, "Fractional time-varying grey traffic flow model based on viscoelastic fluid and its application," *Transportation Research Part B: Methodological*, vol. 157, pp. 149–174, 2022.

[14] T. Wang, R. Cheng, and Y. Wu, "Stability analysis of heterogeneous traffic flow influenced by memory feedback control signal," *Applied Mathematical Modelling*, vol. 109, pp. 693–708, 2022.

[15] H. Zhao, G. Zhang, W. Li, T. Gu, and D. Zhou, "Lattice hydrodynamic modeling of traffic flow with consideration of historical current integration effect," *Physica A: Statistical Mechanics and Its Applications*, vol. 503, pp. 1204–1211, 2018.

[16] F. Sun, A. H. F. Chow, S. M. Lo, and H. Ge, "A two-lane lattice hydrodynamic model with heterogeneous lane changing rates," *Physica A: Statistical Mechanics and Its Applications*, vol. 511, pp. 389–400, 2018.

[17] C. Zhu, S. Zhong, and S. Ma, "Two-lane lattice hydrodynamic model considering the empirical lane-changing rate," *Communications in Nonlinear Science and Numerical Simulation*, vol. 73, pp. 229–243, 2019.

[18] G. Zhang, "Study on varying time delay on traffic stability in a novel lattice hydrodynamic model," *Physica A: Statistical Mechanics and Its Applications*, vol. 505, pp. 1103–1112, 2018.

[19] P. Redhu and A. K. Gupta, "Jamming transitions and the effect of interruption probability in a lattice traffic flow model with passing," *Physica A: Statistical Mechanics and Its Applications*, vol. 421, pp. 249–260, 2015.

[20] D. H. Sun, G. Zhang, M. Zhao, S. L. Cheng, and J. D. Cao, "Stability analysis of feedforward anticipation optimal flux difference in traffic lattice hydrodynamic theory," *Communications in Nonlinear Science and Numerical Simulation*, vol. 56, pp. 287–295, 2018.

[21] C. Zhai and W. T. Wu, "An extended continuum model with consideration of the self-anticipative effect," *Modern Physics Letters B*, vol. 32, no. 8, Article ID 1850382, 2018.

[22] X. Li, K. Fang, and G. Peng, "A new lattice model of traffic flow with the consideration of the drivers' aggressive characteristics," *Physica A: Statistical Mechanics and Its Applications*, vol. 468, pp. 315–321, 2017.

[23] R. Cheng, H. Ge, and J. Wang, "An extended continuum model accounting for the driver's timid and aggressive attributions," *Physics Letters A*, vol. 381, no. 15, pp. 1302–1312, 2017.

[24] C. Zhai and W. Wu, "Analysis of drivers' characteristics on continuum model with traffic jerk effect," *Physics Letters A*, vol. 382, no. 47, pp. 3381–3392, 2018.

[25] C. Zhai, W. Wu, W. Liu, and L. Huang, "Modeling and simulation of traffic flow mechanics based on cognitive differences," *Transportation system engineering and information*, vol. 18, no. 06, pp. 152–160, 2018.

[26] C. Zhai and W. Wu, "Stability analysis of two-lane lattice hydrodynamic model considering lane-changing and memorial effects," *Modern Physics Letters B*, vol. 32, no. 20, Article ID 1850233, 2018.

[27] C. Zhai and W. Wu, "Car-following model based delay feedback control method with the gyroidal road,"

International Journal of Modern Physics C, vol. 30, no. 09, Article ID 1950073, 2019.

[28] R. Cheng, J. Wang, H. Ge, and Z. Li, "Nonlinear analysis of an improved continuum model considering headway change with memory," *Modern Physics Letters B*, vol. 32, no. 03, Article ID 1850037, 2018.

[29] R. Cheng and Y. Wang, "An extended lattice hydrodynamic model considering the delayed feedback control on a curved road," *Physica A: Statistical Mechanics and Its Applications*, vol. 513, pp. 510–517, 2019.

[30] J. Zhou and Z. K. Shi, "A modified full velocity difference model with the consideration of velocity deviation," *International Journal of Modern Physics C*, vol. 27, no. 06, Article ID 1650069, 2016.

[31] J. Zhang, T. Q. Tang, and S. W. Yu, "An improved car-following model accounting for the preceding car's taillight," *Physica A: Statistical Mechanics and Its Applications*, vol. 492, pp. 1831–1837, 2018.

[32] C. Zhai and W. Wu, "Stability analysis of the new lattice model considering horn effect and driver heterogeneity," *Journal of Automation*, vol. 8, pp. 1738–1747, 2020.